Demonstration of Model-Independent Control of the Longitudinal Phase Space of Electron Beams in the Linac Coherent Light Source with Femtosecond Resolution

Alexander Scheinker*
Los Alamos National Laboratory

Dorian Bohler
Stanford Linear Accelerator Center
(Dated: February 20, 2018)

The dynamics of intense electron bunches in free electron lasers and plasma wakefield accelerators are dominated by complex collective effects such as wakefields, space charge, coherent synchrotron radiation, and drift unpredictably with time, making it extremely difficult to control and tune for specific beam properties using traditional model-based approaches. We report on the first of its kind automatic, model-independent feedback-based control of the longitudinal phase space (energy and charge density distribution) of the electron beam at the Linac Coherent Light Source at femtosecond resolution. Feedback is performed based only on x-band transverse deflecting cavity measurements made at the end of the accelerator. Automatic tuning of six coupled beam line components (linac phase and bunch compressor energy set points), transforming initial electron bunches of length ∼300 fs to match desired ∼80 fs long current profiles while also matching desired energy spread profiles.

Free electron lasers (FEL) and plasma wakefield accelerators (PWFA) are extremely powerful scientific instruments due to their flexibility to provide a wide ranges of beam energies and bunch lengths for various experiments. For example, the Linac Coherent Light Source (LCLS) FEL provides users with photon energies ranging from 0.27 keV to 12 keV based on electron bunch charges and pulse durations ranging from 20 pC at 3 fs to 1 nC at 300 fs [1–3]. The updated PWFA facility for advanced accelerator experimental tests (FACET-II) is planning to provide bunch charges ranging from pC to nC of either positron or electron beams at energies of 1 to 10 GeV [4].

Precise control of bunch lengths, current profiles, and energy spreads of increasingly shorter electron beams at femtosecond resolution is extremely important and challenging [5, 6]. Traditional model-based approaches are severely limited by uncertain and time varying beam phase space distributions, misalignments, thermal cycling, time varying parameters, and collective effects such as space charge forces wakefields, and coherent synchrotron radiation extremely short high current bunches. For example, reconfiguring the LCLS to a low charge mode in order to provide 3 fs bunches can take up to 10 hours of manual tuning by experienced operators and beam line physicists. Such difficulties are limiting both the complexity of beam arrangements that can be explored at these facilities and wasting valuable, extremely limited beam time. These difficulties will only grow with for future facilities such as LCLS-II where new and exotic schemes such as two-color operation are being explored [7, 8], or FACET-II which is planning on providing custom tailored current profiles [9].

Our adaptive, model-independent approach is based on a recently developed method [10], which has been utilized for predicting and tracking longitudinal phase space distributions at the PWFA FACET [11] and has been analytically studied for a large class of nonlinear, time-varying dynamics systems [12].

The method is applicable to n-dimensional dynamic system of the form

$$\frac{d\mathbf{x}}{dt} = f(\mathbf{x}, \mathbf{p}, t), \tag{1}$$

where $\mathbf{x} = (x_1, \ldots, x_n)$ are physical quantities such as the beam properties at a specific location in a particle accelerator, $\mathbf{p} = (p_1, \ldots, p_m)$ are controlled parameters, t is time, and the function f may be an unknown function governing the system's dynamics. We simultaneously tuned six parameters, $\mathbf{p} = (p_1, \ldots, p_6)$, of the LCLS beam line as shown in Figure 1 in red:

1. The Linac 1 (L1S) phase set point has an influence on both the electron bunch energy and the bunch length change created by the bunch compressor BC1. L1S drifts continuously due to temperature and in normal operation has to be corrected via a lengthy, invasive phase scan. Within a limited range, a feedback system adjusts L1S automatically to maintain a desired bunch length.

2. The Linac 1 X-band (L1X) linearizing cavity phase set point linearizes the electron bunch, compensating for energy offsets introduced by L1S.

3. The bunch compressor 1 (BC1) energy set point determines the amount of longitudinal compression of the bunch and provides feedback for the L1 amplitude set point.

4. The Linac 2 (L2) phase set point controls a group of multiple klystrons, effects bunch length, and suffers from the same drifts as L1.

5. Bunch compressor 2 (BC2) energy set point. BC2 is a second stage of compression at higher energy.

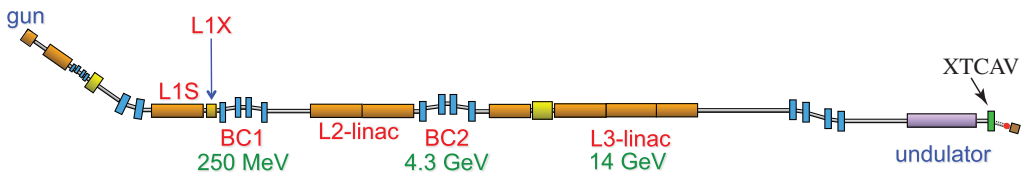

FIG. 1. Simple overview of LCLS showing the controlled parameters and XTCAV diagnostic location.

6. Linac 3 (L3) phase set point. L3 is another multi-klystron system with phase and amplitude drifts.

Our goal was to minimize a measurable, but analytically unknown "cost function," $C(\mathbf{x}(\mathbf{p},t),t)$, by adjusting the parameters $\mathbf{p}$ without a knowledge of the analytic form of C. In this work $C(\mathbf{x}(\mathbf{p},t),t)$ was a weighted sum of the difference between measured current $\hat{\rho}_c(z)$ and energy spread profiles $\hat{\rho}_e(E)$ and desired profiles $\rho_c(z)$ and $\rho_e(E)$ at the end of the FEL, of the form

$$C(\mathbf{x}(\mathbf{p},t),t) = c_1 \int_0^L |\hat{\rho}_c(z) - \rho(z)|\, dz + c_2 \int_{-\Delta E}^{\Delta E} |\hat{\rho}_e(E) - \rho_e(E)|\, dE, \quad (2)$$

where L is the length of the electron bunch and $E \in [-\Delta E, \Delta E]$ is the range of electron energy within the bunch. Typically, in practice we only have access to noise corrupted measurements of C of the form

$$y = C + n(t). \quad (3)$$

For this experiment, we used the x-band transverse deflecting cavity (XTCAV) to streak the beam. The XTCAV rotates the electron bunch, translating longitudinal position to transverse position. The rotated bunch is then passed through a vertical dipole causing an energy-dependent curvature of the electron trajectory. The setup is shown in Figure 2, providing both longitudinal bunch current profile and energy distribution [13].

We adjust the parameters p_j according to the rule

$$\frac{dp_j}{dt} = \sqrt{2\alpha\omega_j}\cos(\omega_j t + ky), \quad (4)$$

where $\omega_j = \omega r_j$ and $r_j \neq r_i$ for $i \neq j$. The term $\alpha > 0$ can be thought of as the dithering amplitude and can be increased to escape local minima. Once the dynamics have settled a parameter p_j will oscillating about a local minimum with amplitude $\sqrt{\alpha/\omega_j}$. The term $k > 0$ is the feedback gain. For large ω, the dynamics of (4) are given, on average, by the simple dynamics

$$\frac{d\mathbf{p}}{dt} = -k\alpha\left(\nabla_{\mathbf{p}} C(\mathbf{x}(\mathbf{p},t),t)\right)^T, \quad (5)$$

a gradient descent of the actual, analytically unknown function C although the feedback is based only on the noisy measurements $y(t)$. Intuitively, the reason behind this convergence is that by dithering each parameter at a unique frequency the evolution of the parameters has been made orthogonal in Hilbert space in the form of the $L^2[0,t]$ inner product:

$$\lim_{\omega_1,\omega_2\to\infty} \int_0^t \cos(\omega_1\tau)\cos(\omega_2\tau)d\tau = 0, \quad (6)$$

see [10, 12] for more details.

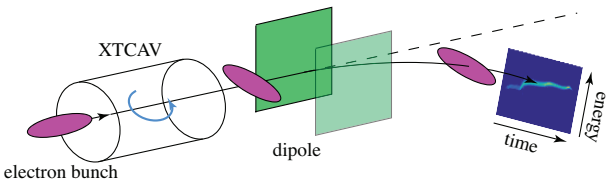

FIG. 2. Transverse deflecting radio frequency structures horizontally streak the beam before it is deflected by a vertical dipole into the detector, measuring both the longitudinal current profile and energy spread.

Although the resulting dynamics on-average perform a gradient descent of a time-varying, unknown function, this approach has many advantages over a standard gradient descent-type search: 1). This continuous, dynamic method can tune many parameters of unknown, nonlinear, open-loop unstable systems, simultaneously without exponential growth in the number of computations required. 2). The method is robust to measurement noise and external disturbances and can track quickly time-varying parameters. 3). Although operating on noisy and analytically unknown systems, the parameter updates have analytically guaranteed constraints:

$$\left|\frac{dp_j}{dt}\right| = \left|\sqrt{2\alpha\omega_j}\cos(\omega_j t + ky)\right| \leq \sqrt{2\alpha\omega_j}, \quad (7)$$

which make it safe for in-hardware implementation.

We began by recording XTCAV distribution measurements for a fixed set of parameters, which would serve as our desired profiles $\rho_c(z)$ and $\rho_e(E)$. We then changed parameter settings and thereby the beam's phase space distributions and started the algorithm in order to automatically recover the desired profiles. The procedure of applying (4) iteratively in hardware is done via the finite difference approximation:

$$p_j(n+1) = p_j(n) + \Delta\sqrt{2\alpha\omega_j}\cos(\omega_j n\Delta + ky(n)) \quad (8)$$

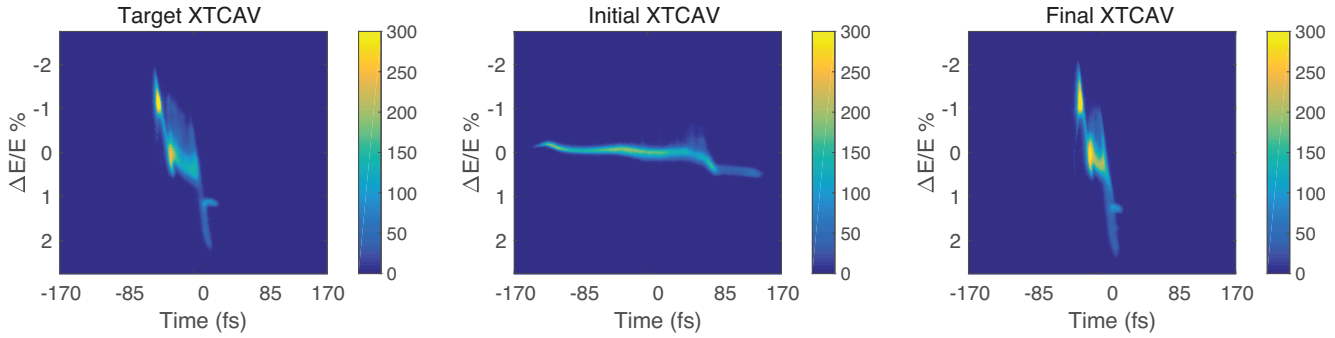

FIG. 3. First experiment: initial, final, and matched phase space distributions shown with an arbitrary intensity scale.

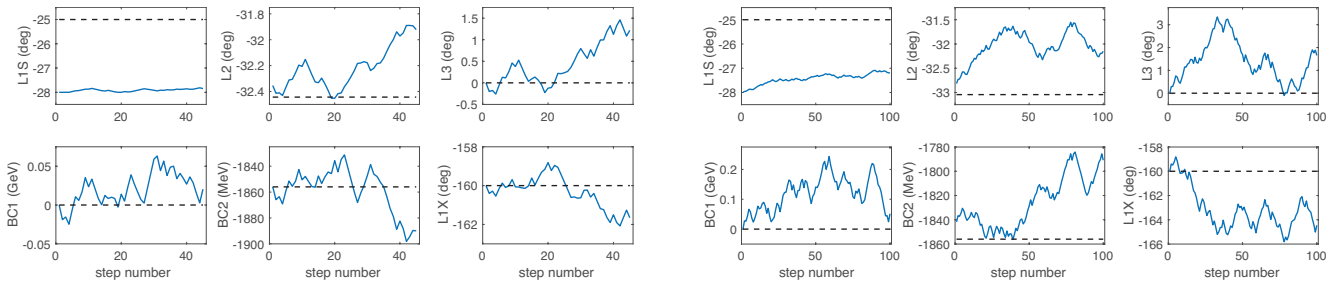

FIG. 4. Evolution of the parameters being tuned by the ES algorithm. Left: first experiment where only L1S phase was changed. Right: second experiment where L1S and L2 phases and BC2 energy set points were changed.

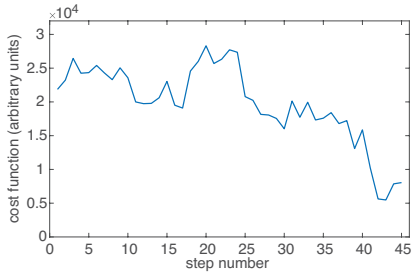

FIG. 5. First experiment, evolution of the cost function.

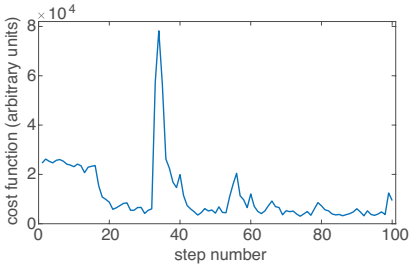

FIG. 7. Second experiment, evolution of the cost function.

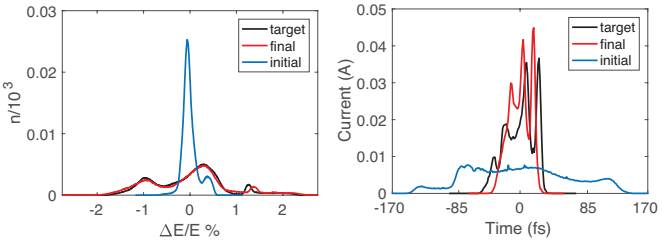

FIG. 6. First experiment, matched current and energy profiles.

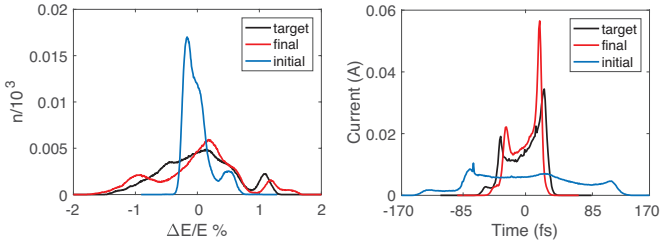

FIG. 8. Second experiment, matched current and energy profiles.

which is accurate for $\Delta < \frac{2\pi}{\max\{\omega_j\}} \ll 1$. The iterative procedure is started with initial parameter settings $\mathbf{p}(1)$, after which the XTCAV image is recorded and projected on the vertical and horizontal axes. The raw measurements are smoothed with a ten point moving average filter and the current profile $\hat{\rho}_c(z)$ and the energy spread profile $\hat{\rho}_e(E)$ are then used to determine the cost, $C(1)$ as given by (2). Based on $C(1)$, new parameter settings $\mathbf{p}(2)$ are determined according to (8). The process is continued iteratively, at a rate of 1/4 Hz to allow for all

directed parameter changes to settle.

In the first experiment, only the phase set point of L1S was changed by -3 deg, causing a significant change in both bunch length and energy spread. Figure 3 shows the desired, initial, and final longitudinal phase space distributions as achieved by the automatic tuning algorithm. We then allowed the iterative procedure to automatically re-tune all six parameters in order to recover the desired distributions. The evolution of all 6 parameters is shown on the left side of Figure 4 and the evolution of the cost function is shown in Figure 5. Although the cost function is minimized, it is clear from Figure 4 that the L1S phase did not return to its original value, but was compensated by changes in the phases of L1X, L2, L3 and the energy set point of BC2. This demonstrates the complexity of the tuning problem which does not have a unique solution. Figure 6 shows the desired, initial, and final distributions, $\rho_c(z)$ and $\rho_e(E)$, based on which the cost function values were calculated. The energy spread distribution has been matched almost exactly, while the current profile has recovered the correct bunch width, but is limited in accuracy in terms of the high frequency characteristics because of the 10-point moving average that was used to clean up the profiles. Running at 1/4 Hz, the total tuning time in the first experiment was 3 minutes.

In a second experiment, the L1S and L2 phase and BC2 energy set points were modified and the iterative scheme was again able to re-match the distributions by adjusting all parameters. Evolution of the cost function and the final distributions are shown in Figures 7 and 8, respectively. The large jump in cost function value see in Figure 7 is due to a temporary drop out of the beam, during which we kept running and recording blank XTCAV images, demonstrating the robustness of the scheme to noise and sudden step changes. The second experiment shows a better match of current profiles and a worse match in energy spread distributions. The total tuning time in the second experiment was ∼6.6 minutes for 100 setps, although, as can be seen by the cost function value, the feedback had actually converged within ∼ 20 steps. In practice, besides for switching between different phase space distributions, this feedback could be run continuously on one or multiple components in order to maintain desired beam properties despite uncertain, time-varying drift of machine components which usually results in periodic re-calibrations.

These preliminary results have demonstrated a new approach to controlling the longitudinal phase space of high energy, short, electron bunches. The major strength of this approach is that it is model independent and robust to noise and therefore it was possible to apply it as a feedback loop on LCLS and not just for simulation studies. However, because the averaged dynamics or on average performing a gradient descent, one limitation is that the scheme can get stuck in local minima. In fact both of these experiments demonstrated a finding of a local minimum in 6 parameter space which very closely matched both the energy and current profiles, but not perfectly both simultaneously.

The next step in this work is to add more controlled parameters, such as electron bunch charge, and combine this local, real-time feedback method with global machine learning (ML) based approaches. Powerful ML-based tools such as neural networks can be trained to automatically tune and control large complex systems such as particle accelerators [14]. However, machine learning approaches alone are insufficient for such systems because they are time-varying and so their learned characteristics are always drifting. In future work we plan on combining this algorithm with machine learning by allowing a sufficiently trained neural network to bring parameters within a close neighborhood of their optimal settings for a given desired phase space distribution, and then allowing the method described here to zoom in, via feedback and track the actual optimal settings.

The algorithm presented here is completely general, adjusting a high dimensional parameter space based only scalar "cost" value measurements and therefore can be useful for any large, complex system. In particular, PWFA facilities, such as the planned FACET-II can benefit from the beam control approach demonstrated here for creating custom shaped electron bunches.

This research was supported by The Los Alamos National Laboratory and The Stanford Linear Accelerator Center.

* ascheink@lanl.gov

[1] P. Emma *et al.*, Nat. Photonics **4.9**, 641 (2010).
[2] Y. Ding *et al.*, Phys. Rev. Lett. **102.25**, 254801 (2009).
[3] D. Ratner *et al.*, Phys. Rev. Lett. **114.5**, 054801 (2015).
[4] C. Joshi *et al.*, Plasma Physics and Controlled Fusion **60.3**, 034001 (2018).
[5] R. Akre *et al.*, SLAC-PUB- 16643, 2016.
[6] T. J. Maxwell *et al.*, Phys. Rev. Lett. **111.18**, 184801 (2013).
[7] A. A. Lutman *et al.*, Nat. Photonics **10.11**, 745 (2016).
[8] T. O. Raubenheimer in *Proceedings of the International Particle Accelerator Conference*, Richmond, VA, USA, 2015.
[9] V. Yakimenko *et al.*, in *Proceedings of IPAC2016*, Busan, Korea, 2016.
[10] A. Scheinker in *Proceedings of the 2013 International Particle Accelerator Conference*, Shanghai, China, 2013.
[11] A. Scheinker *et al.*, Phys. Rev. ST Accel. Beams **18 (10)**, 102801 (2015).
[12] A. Scheinker *et al.*, International Journal of Robust and Nonlinear Control **28(2)**, 568-581 (2018).
[13] C. Behrens *et al.*, Nat. Commun **5**, 3762 (2013).
[14] A. L. Edelen *et al.*, IEEE Trans. on Nucl. Science **63.2**, 878-897 (2016).